Spin-transfer torque and anisotropy in Fe/Ag/Fe spin-torque oscillators

R. Lehndorff, D. E. Bürgler, A. Kákay, R. Hertel, C. M. Schneider

IFF-9: Electronic Properties

Current-driven magnetization dynamics in spin-torque oscillators (STOs) has strong potential for high-frequency (HF) applications. We investigate the influence of magnetocrystalline anisotropy on the current-driven magnetization dynamics in single-crystalline Fe/Ag/Fe(001) STOs. The four-fold in-plane anisotropy of the Fe(001) films stabilizes the 90°-state with perpendicular magnetizations in addition to parallel and antiparallel alignment. The current-driven dynamics in the 90°-state is governed by the interplay between spin-transfer torque and anisotropy and enables a steady-state precession of the free magnetization at low applied magnetic field. Thus, we demonstrate a new route to realize STNOs operating without applying an external field.

High current densities passing through magnetic nanostructures can induce magnetization switching or excite steady-state oscillations. These phenomena are due to spin angular momentum transfer from spin-polarized currents to the magnetization, where it acts as the so-called spin-transfer torque (STT). Generation of HF signals in STOs is promising for applications in communication technology. In standard STOs a strong externally applied magnetic field is required to prevent switching and to stabilize the steady-state precessional motion [1]. This external magnetic field, however, imposes problems for the application of STOs. Recently presented possibilities to circumvent the necessity of an external field rely on shaping the spin accumulation by suitable material combinations [2] or on exploiting the shape anisotropy of elliptically shaped free layers [3]. Here we present a third possibility [4] by employing a strong internal magnetic field instead of the external field. In our single-crystalline Fe/Ag/Fe(001) nanopillars the magnetocrystalline anisotropy of bcc-Fe results in an effective field with four-fold in-plane symmetry. The total torque –the sum of STT and effective field induced torque– that finally acts on the magnetization has a local minimum when the relative angle ϑ of the two magnetizations is 90°. In the vicinity of this minimum a zero-field precession is possible.

We fabricate our STOs by applying a combined optical and e-beam lithography process to 1 nm Fe (seed layer), 150 nm Ag (buffer layer), 20 nm Fe (fixed layer), 6 nm Ag (interlayer), 2 nm Fe (free layer), and 50 nm Au (capping layer) multilayers grown by molecular beam epitaxy [5]. The final nanopillar as sketched in Fig. 1(a) has a circular cross-section with a diameter of 70 nm [Fig. 1(b)].

Resistance *versus* DC current measurements [Fig. 1(c)] starting in a low resistive state show a two-step switching at positive currents to an intermediate and high resistive level. The magnetization of the free layer (red arrow) first switches from a parallel to a 90°-orientation relative to the fixed layer magnetization (green arrow). In a second step at a larger current it finally switches to an antiparallel alignment. A similar behavior is observed for the sweep to negative currents. Figure 2 shows HF spectra taken at a low field of 5 mT for applied DC currents corresponding to the intermediate resistive 90°-state [red marked current range in Fig. 1(c)]. Note that 5 mT are much weaker than the anisotropy field and, thus, the HF signals can also be observed at zero field. With currents increasing from 6.0 to 6.75 mA the frequency increases from 6.93 to 7.04 GHz yielding a mode agility of 150 MHz/mA.

We perform macrospin simulations by numerically solving the Gilbert equation. In order to describe the current-driven magnetization dynamics, we use the

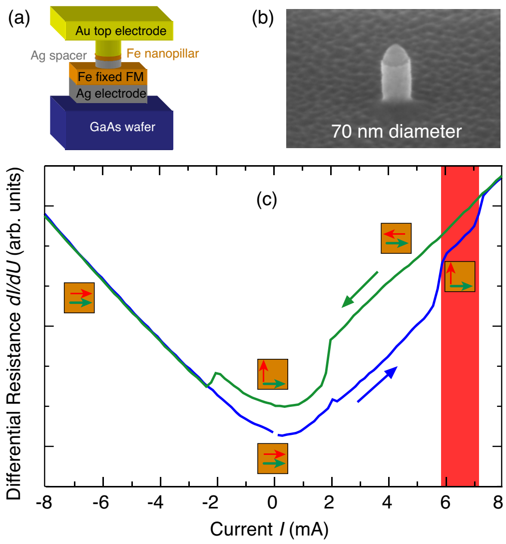

FIG. 1: (a) Sample structure. (b) SEM micrograph of the nanopillar after etching. (c) Resistance versus *DC current measured at 5 K with a weak in-plane magnetic field of 7.9 mT along an easy axis of the Fe layers.*

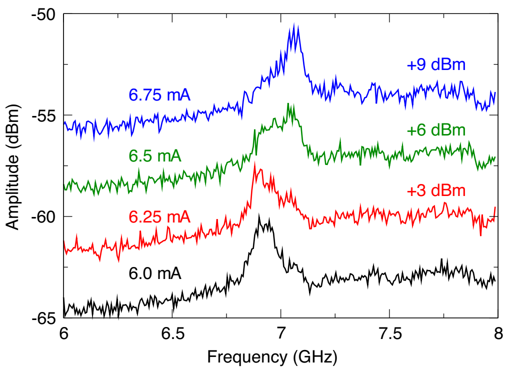

FIG. 2: Microwave spectra recorded at 5 K and in a weak field of 5 mT. All curves are taken at DC currents corresponding to the 90°-state [red area in Fig. 1(c)].

version expanded by the STT term as introduced by Slonczewski [6]:

$$\frac{d\vec{m}}{dt} = -\gamma\vec{m}\times\vec{H}_{\text{eff}} + \alpha\vec{m}\times\frac{d\vec{m}}{dt} + j\cdot g(\vartheta)\cdot\vec{m}\times(\vec{m}\times\vec{p}), \quad (1)$$

where $\vec{m}$ is the normalized magnetization vector, γ the gyromagnetic ratio, $\vec{H}_{\text{eff}}$ the effective field, α the Gilbert damping constant, j the current density, $\vec{p}$ the direction of the fixed layer magnetization, and $g(\vartheta)$ the STT efficiency with ϑ the angle between $\vec{m}$ and $\vec{p}$. We use $g(\vartheta)$ given in [7] based on more advanced calculations compared to the often used results from [6]:

$$g(\vartheta) = \frac{\hbar P\Lambda}{4e}\frac{1}{\Lambda\cos^2(\vartheta/2)+\Lambda^{-1}\sin^2(\vartheta/2)}, \quad (2)$$

where P is the spin polarization and Λ the asymmetry parameter as defined in Ref. [7]. For Fe/Ag/Fe(001) $\Lambda = 1.6\ldots3.4$ clearly deviates from unity [8]. Therefore, the maximum torque according to Eq. (2) occurs for $\vartheta > 90°$ [Fig. 3(a)]. Figure 3(b) shows simulations of the low-field precession enabled by the anisotropy. The magnetization of the free layer $\vec{m}$ is initially oriented along the $+y$-direction and, thus, perpendicular to the fixed layer magnetization. Red arrows indicate the direction and strength of the effective-field dependent damping torque and the blue arrows represent the STT. For $m_x < 0$ [right half of Fig. 3(b] they point away from the precession axis and act as an excitation, where as for $m_x > 0$ [left half of Fig. 3(b)] the STT acts as a damping. The net action of the STT during one precessional cycle seems to vanish. However, the STT is asymmetric with respect to the direction of the precession axis (the $+y$-direction), *i.e.* the STT on the right side are stronger than on the left. Therefore, the net action of the STT does not vanish, which is essential for this dynamic mode. For increasing current density the net action of the STT dominates over damping and a steady-state precession can be sustained. The precession axis slightly shifts to $m_z > 0$. This results in a non-zero mean demagnetizing field contributing to $\vec{H}_{\text{eff}}$ and, therefore, increases the precession frequency for increasing current strength as observed in Fig. 2. Due to the partial cancelling of the STT the cone angle of the precession is relatively small, but the low-field precession covers the region of the GMR(ϑ) curve with the steepest gradient and therefore results in measurable microwave signals (Fig. 2).

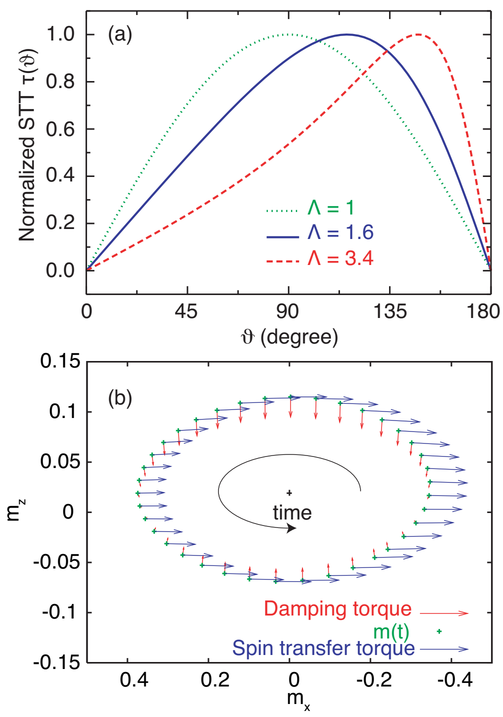

FIG. 3: (a) Angular dependence of the STT amplitude $g(\vartheta)\sin(\vartheta)$ according to Eq. (2) for different Λ. (b) Representation of the STT (blue arrows) and damping torque (red arrows, enlarged by factor 5 relative to the STT) for the low-field precession in the 90°-state.

In conclusion, the low-field HF excitations found in the 90°-state demonstrate a new route to realize spin-transfer oscillators without the need for applying strong external magnetic fields.

[1] S. I. Kiselev, J. C. Sankey, I. N. Krivorotov, N. E. Emley, R. J. Schoelkopf, R. A. Buhrman, and D. C. Ralph, Nature **425**, 380 (2003).

[2] O. Boulle, V. Cros, J. Grollier, L. G. Pereira, C. Deranlot, F. Petroff, G. Faini, J. Barnas, and A. Fert, Nature Physics **3**, 492 (2007).

[3] T. Devolder, A. Meftah, K. Ito, J. A. Katine, P. Crozat, and C. Chappert, J. Appl. Phys. **101**, 063916 (2007).

[4] R. Lehndorff, D. E. Bürgler, A. Kakay, R. Hertel, and C. M. Schneider, IEEE Trans. Magn. **44**, 1951 (2008).

[5] H. Dassow, R. Lehndorff, D. E. Bürgler, M. Buchmeier, P. A. Grünberg, C. M. Schneider, and A. van der Hart, Appl. Phys. Lett. **89**, 222511 (2006).

[6] J. C. Slonczewski, J. Magn. Magn. Mater. **159**, L1 (1996).

[7] J. C. Slonczewski, J. Magn. Magn. Mater. **247**, 324 (2002).

[8] R. Lehndorff, D. E. Bürgler, A. Kakay, R. Hertel, and C. M. Schneider, Phys. Rev. B **76**, 214420 (2007).